Department of physics, École Normale Supérieure, Paris

Swiss Plasma Center, EPFL, Lausanne

Turbulence characterization
In magnetically confined fusion research

Master Thesis 2024

Andrea Combette

Supervisors:

Dr Mr. Oleg Krutkin **Pr. Jean François Allemand**

Cautionary note : This paper is a report on numerical methods for the shallow water equations and gravity waves. It is not intended to be a complete and rigorous study of the subject. The reader is invited to refer to the references for further details. It has been made by a Master Student, with some background in physics and mathematics, but no prior knowledge of the subject. It is therefore not intended to be a reference for experts in the field.

Contents

1 Theoretical Background **4**
I Nuclear Fusion . . . 4
1 Reaction . . . 4
a D-T reaction . . . 4
b Fusion Cross-section . . . 4
c Energy balance and Lawson criterion . . . 4
2 Tokamak . . . 4
II Wave propagation in plasma . . . 5
1 Plasma as a medium . . . 5
2 Wave equation . . . 5
3 Dispersion relation . . . 5
a Ordinary mode . . . 5
b Extraordinary mode . . . 5
III Plasma Turbulence . . . 5
1 Characterization . . . 5
2 Diagnostics . . . 5
a Doppler Reflectometry . . . 5
b RCDR . . . 5
c Short Pulse Reflectometry . . . 5

2 Linear Regime Study **5**
I 1 dimensional study . . . 5
1 Perturbed Density Profile . . . 5
a Step-like perturbation . . . 5
a.1 Model . . . 5
a.2 statistical approach . . . 5
b Gaussian-like perturbation . . . 5
II 2 dimensional study . . . 6
1 Numerical Integration for plasma density . . . 6
2 Full wave Modelling . . . 6
3 Background profiles . . . 6
III Numerical Integration . . . 7
1 statistical Properties of the delay . . . 7
2 Pulse shape Study . . . 7
3 Gaussian fitting of the pulse . . . 10
IV Model collapses . . . 10
V Datasets building . . . 11

3 Mathematical appendix **12**

Abstract

One of the common goals in experimental magnetically confined fusion research is characterization of the plasma turbulence. To that end, TCV tokamak features a novel short-pulse reflectometry (SPR) diagnostic, which can potentially be utilized to measure properties of the turbulence. It is essentially a radar system, where the plasma is probed by a short (under ns) microwave pulse in the presence of the cut-off (reflection) area from which the pulse reflects back into the probing antenna. The position of the cut-off for a particular probing frequency (in 50-75 GHz) range is determined by the plasma electron density. Thus, by measuring the delay between probing and reflected beam corresponding to different probing frequencies, the information about the electron density profile is inferred including its turbulent perturbations. Unfortunately, the complex interaction of microwaves with magnetized plasma makes it difficult to establish the connection between SPR measurements and properties of the turbulence. Numerical modeling utilizing the synthetic diagnostic approach was carried out to establish this connection for the case of low turbulence amplitudes (linear regime). However, the case of large turbulence amplitudes (nonlinear regime) is yet to be explored. Within the project a systematic analysis of the SPR diagnostic in the nonlinear regime will be carried out. The numerical finite difference code CUWA, which solves the wave equation for a given plasma density and provides synthetic reflected pulse will be utilized. The main goal of the project is identifying markers that can be used to determine if the diagnostic is operating in the nonlinear regime and assessing the possibility of determining the turbulence parameters regardless. Time permitting, the results of this analysis will be applied to the interpretation of experimental measurements and possibly used to develop a machine learning approach to analyzing SPR data.

1

Theoretical Background

I Nuclear Fusion

The nuclear fusion reaction is the process by which two light atomic nuclei combine to form a heavier nucleus. It is accompanied by the release or absorption of energy depending on the masses of the nuclei involved. Indeed, the more the nuclei are light, the more energy is released due to the overcoming short-range nuclear force for light nuclei. However, to overcome the Coulomb barrier the reactant must be sufficiently close for a long enough time to allow the quantum tunnel effect between both particles. To do so, we must heat up the reactant to huge temperatures such that these latter are starting ionizing and turning into plasma.

1 Reaction

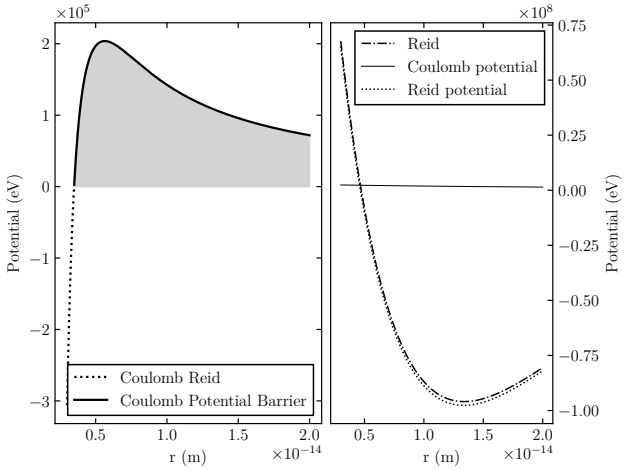

Figure 1.1: Here we plot the residual Coulomb potential barrier between two proton considering the strong nuclear force as the Reid potential [cite]. On the right, the residual Reid potential.

Here it appears that the thermal energy needed to overcome the coulomb barrier is about :

$$E_{\text{thermal}} \approx 0.2\text{MeV}.$$

This corresponds to a temperature of $2.5e^9$ K, This is the reason why we need to heat up the plasma to such high temperatures. Note that the quick considerations are for proton-proton interaction, in fact the thermal energy needed is much smaller around $1e^8$ K for the deuterium-tritium reaction, due to quantum tunneling effect, and screening of coulomb potential by other nucleons:

a D-T reaction

At the TCV the studied reaction is the deuterium-tritium reaction, which is the most promising reaction for fusion power, Indeed the energy barrier for the reaction to happen is about 70 keV, whereas for deuterium-deuterium reaction it's 0.1MeV,and for the deuterium-Helium it's about 0.2MeV. The reaction is the following:

$$\mathrm{D}^2 + \mathrm{T}^3 \rightarrow \mathrm{He}^4 + \mathrm{n}(17.6\text{ MeV})$$

The liberated energy is big enough to sustain the reaction, but it has a given probability to happen, and a positive energy yield is necessary to use the nuclear fusion reaction. A possible measure of this probability is the fusion cross-sectional area, which is much more that just a geometrical cross-section.

b Fusion Cross-section

The fusion cross section is enhanced by the tunneling effect transparency (T) and by the reaction characteristics R. It is given by the following formula :

$$\sigma \approx \sigma_{\text{geometry}} \times T \times R,$$

where σ_{geometry} is the geometrical cross-section, T is the tunneling effect transparency, and R is the reaction characteristics. The tunneling effect transparency is given by the Gamow factor, and the reaction characteristics given by the astrophysical S-factor.

c Energy balance and Lawson criterion

$\tau_E = \frac{W}{P_{\text{loss}}}$

For the deuterium–tritium reaction, the physical value is at least

$$n\tau E \geq 1.5.10^{20} \frac{\text{s}}{\text{m}^3}$$

Different regimes of confinement : Magnetic, Inertial, ...

2 Tokamak

Magnetic confinement, plasma physics, ...

II Wave propagation in plasma

1 Plasma as a medium

2 Wave equation

3 Dispersion relation

a Ordinary mode

b Extraordinary mode

III Plasma Turbulence

1 Characterization

instabilities grow due to inverse cascade of energy (2D geometry) –> scale

2 Diagnostics

a Doppler Reflectometry

b RCDR

c Short Pulse Reflectometry

2

Linear Regime Study

I 1 dimensional study

Assuming a simple plasma density profile $n(x)$, we can study the wave propagation in the plasma. The goal of this approach is to find a way to link the plasma density perturbations to the reflected pulse delay. To retrieve some information about the pulse delay we will use a statistical approach to get rid of the randomness implies by the perturbations considerations. The delay of the probing wave is given by the following formula :

$$\tau_c = 2\int_0^L \frac{dx}{v_g}$$

Where v_g is the group velocity of the wave, L is the position of the cut-off. From the simple assumption $\langle \delta n \rangle = 0$ for an Ordinary mode the v_g expression obtained [] can be used to expand the integral to the following :

$$\frac{2}{c}\int_0^L \frac{dx}{\sqrt{1-\frac{x}{L}-\frac{\delta n}{n_c}}}$$

The main contribution of this integral comes from the vicinity of the cut-off layer, Where the group velocity is the smallest. We can discuss the relevance of this expansion this the main contribution of the integral comes from the cut-off region where the WKB approximation cannot be applied.

1 Perturbed Density Profile

a Step-like perturbation

a.1 Model The apparent divergence of the integral can be tackled using a simple step-like perturbation density profile. With a step-size perturbation characterized by l_{cx} length. This allows to get an analytical expression of the integral for different density profile. However, to get this simplification, we need to assume that the perturbation is small enough such that the WKB approximation can be applied. This is the case for the linear regime, where the perturbation is small enough such that the cut-off layer is not too much perturbed (i.e $\delta_x \ll l_{cx}$). In the case of a large perturbation, an other step perturbation localized far from the cut-off layer can be used to get the same result, which breaks the main assumption of this approach (see fig.1). It's relatively trivial to obtain the following expression for the delay [cite Krutkin] :

$$\tau_d = \frac{4L}{c} - \frac{2L}{c}\sqrt{\frac{L}{l_{cx}}}\frac{\delta n}{n_c}$$

To test this assumption we can compare the analytical expression with the numerical integration of the wave equation, for numerous gaussian perturbations with characteristics length l_{cx} and amplitude δn. The results are shown in the figure **??**. Some discrepancies are observed for large perturbations, but the analytical expression seems to be a good approximation for small perturbations, except for tiny one [cite]. However, One have to introduce a correction factor to the analytical expression to get a better agreement with the numerical integration. This l_{cx} dependant factor is given has not been studied yep but it highllights the linitations of current 1D model. One way to solve this issue, is to introduce Gaussian perturbation density profile.

a.2 statistical approach The statistical approach is to consider the perturbation as a random variable, and to compute the statistical properties of delay of the probing wave. This approach is relevant for the linear regime, where the perturbation is small enough such that the cut-off layer is not too much perturbed (i.e $\delta_x \ll l_{cx}$). Foe example we can compute the standard deviation of the delay depending on the standard deviation of perturbations. This gives us the following :

$$\sigma_{\tau_d} = \frac{2L}{c}\sqrt{\frac{L}{l_{cx}}}\frac{\sigma_{\delta n}}{n_c}$$

b Gaussian-like perturbation

The gaussian perturbation should be a more realistic approach to the perturbation density profile. However, the integral seems to be more difficult to solve.

Indeed, it takes the following form :

$$\tau_d = \frac{2}{c}\int_0^L \frac{dx}{\sqrt{1-\frac{x}{L}-\frac{\delta n \exp\left(-\frac{(x-L)^2}{8l_{cx}^2}\right)}{n_c}}}$$

First let's note that the main criterion $\delta n_c = n_c \frac{l_{cx}}{L}$ is the same as the previous approach. One way to tackle this integral is to expand the gaussian perturbation profile to the first order in order to obtain a hyperbolic integral. The computation are done in the appendix, and leads to the following expression of the delay :

$$\tau_d = \frac{4L}{c} + \frac{4\sqrt{Ll_{cx}}}{c} + \frac{2}{c}x_0\Big(\log\left(\sqrt{(\frac{K_2}{K_1})^2-1}+\frac{K_2}{K_1}\right) - \log\left(\sqrt{(\frac{K_2^*}{K_1})^2-1}+\frac{K_2^*}{K_1}\right)\Big)$$

Where $x_0 = \sqrt{8\frac{n_c}{\delta n}l_{cx}^2}$ and $K_1 = \sqrt{\left(\frac{x_0}{2L}\right)^2 - 8\left(\frac{l_{cx}}{x_0}\right)^2}$, $K_2 = \left(\frac{l_{cx}}{x_0} - \frac{x_0}{2L}\right)$ and $K_2^* = -\frac{x_0}{2L}$.

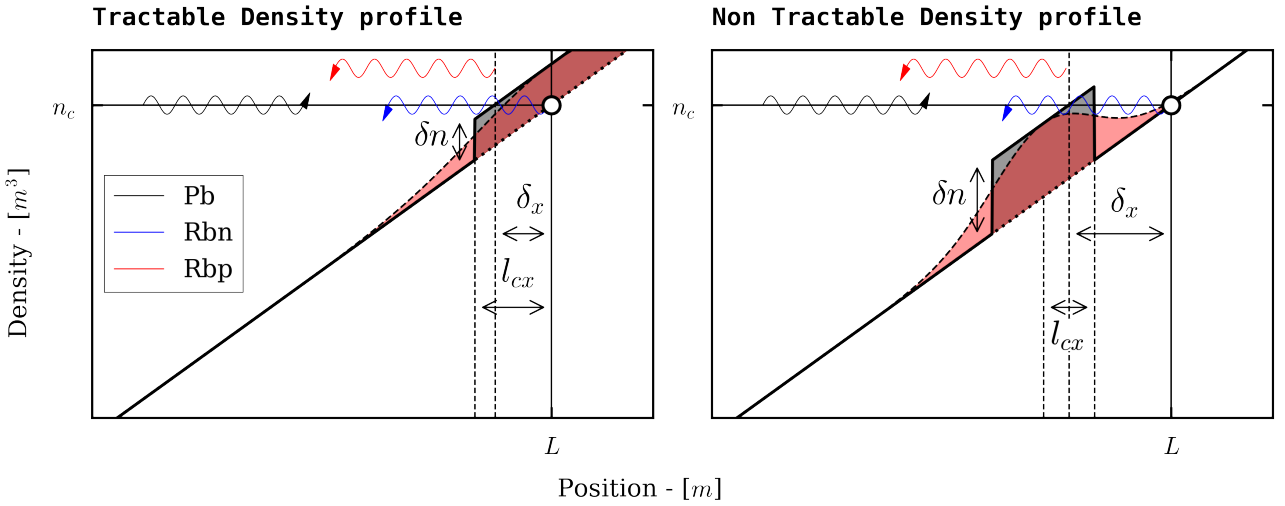

Figure 2.1: Here we plot the density profile of the plasma for different perturbation amplitude, in grey the step-like model perturbation and in coral the gaussian one. For large value density perturbation, the model leads to a contradiction with its assumption, given by a small cut-off layer shift. The gaussian perturbation seems to be a better approach for large perturbation. The blue Pb wave is the probing wave, red Rbp wave is the reflected one and blue Rbn wave is the normal reflected wave, in absence of perturbation.

II 2 dimensional study

The 1D model is a good approximation for small perturbations, but it has some limitations for large perturbations. The 2D model is a more realistic approach, but it is more difficult to solve. The main difficulty comes from the fact that the wave equation is a partial differential equation, and the perturbation density profile is not separable. However, the 2D model can be solved numerically using the finite difference method. The main goal of this approach is to find a way to link the plasma density perturbations to the reflected pulse delay. To retrieve some information about the pulse delay we will use a statistical approach to get rid of the randomness implies by the perturbations considerations.

1 Numerical Integration for plasma density

Kinetic model for plasma, equations ...

2 Full wave Modelling

CUWA CODE : Finite difference method, wave equation, plasma density, ...

3 Background profiles

- For the linear background profile, the global density profile will be the following :

$$n(x,y) = n_c\frac{x}{L} + \delta n(x,y).$$

  WIth δn the 2D gaussian turbulence profile

- For the quadratic background profile L, stands for the gradient scale at the cut-off. Here we choose the following formula to get the value of 1 of the gradient at L, which gives us :

$$n(x,y) = n_c\left[1.25 - \frac{(1.5L_0 - x)^2}{L_0^2}\right] + \delta n(x,y)$$

- One can remark that for small x the turbulence profile is getting preponderant, especially for high amplitudes turbulences, this non realistic

behaviour can be tackled using a linear dependence in the amplitude of the turbulences.

$$n(x,y) = \frac{x}{L}(n_c + \delta n)$$

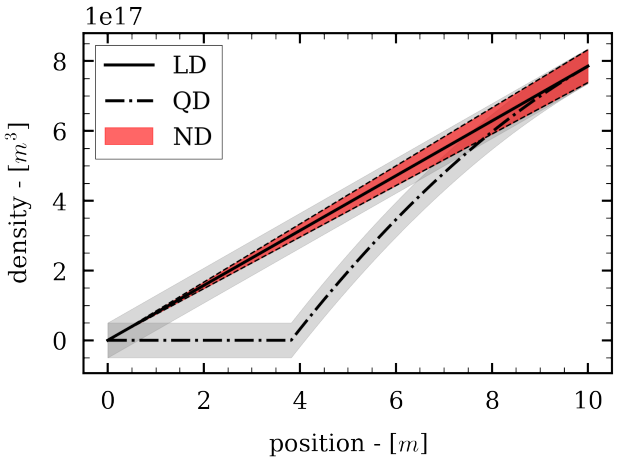

Figure 2.2: Here we plot the three density profile with filled deviation range, in order to see the effect of the linear amplitude dependence of turbulences. **LD** stands for the linear density profile in the following, **QD** for the quadratic one, and **ND** for the linearized turbulence profile

III Numerical Integration

For both 1D and 2D model we can compare the delay rms obtained by integrations, and see if a simple analytical integration of the 1D model can be realistic, which should help releasing some computations time. For the other statistical properties of the delay and the pulse shape, we should limit ourselves to the 2D approach. Which is computationally more expensive, but more realistic. The integration has been done for several background profiles to see if they have strong influence on the probing wave propgation.

1 statistical Properties of the delay

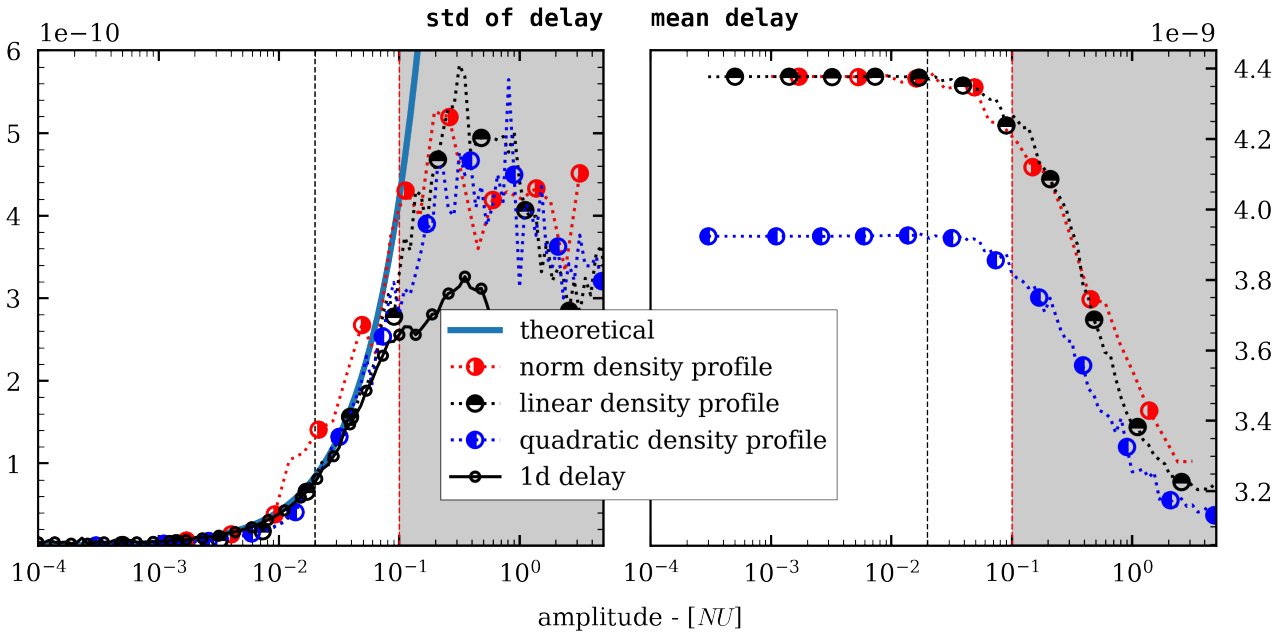

Figure 2.3: Respectively standard deviation of the delay and mean delay evolution. The red vertical line stands for the first critical value unearthed by [], the black one is the second critical value. For both parameter, the analytical expression seems to be a good approximation for small perturbations. For perturbations larger than the first critical value the model collapses has intended, and this for every background profile. We can also note that even if the deviation of the delay has an erratic behavior after the first critical value, the mean delay decrease smooothly. This is strongly related to the displacement of the cut-off layer, indeed the wave is reflected much more quickly due to the presence of strong perturbations.

2 Pulse shape Study

The pulse shape is also an interesting parameter to study, indeed it can give us some information about the plasma density profile, since the pulse shape can be modified by the presence of perturbations due to multiple scattering effects and dispersive effects [see O mode dispersion relation]. The dependance of the pulse shape over the background density profile will be also studied with linear, quadratic and linear modified perturbation profile.

One can expect to have a much larger and randomness dependent pulse, at high turbulence amplitude due to multiple scattering. Indeed the reflected pulse

will be a superposition of all scattered pulse, which should be characterized by a growing tail of the pulse distribution in delay and in width. This can be seen in the figure 2.5.This will be observed on the mean pulse shape, and on the mean statistical parameters of the pulse shape.

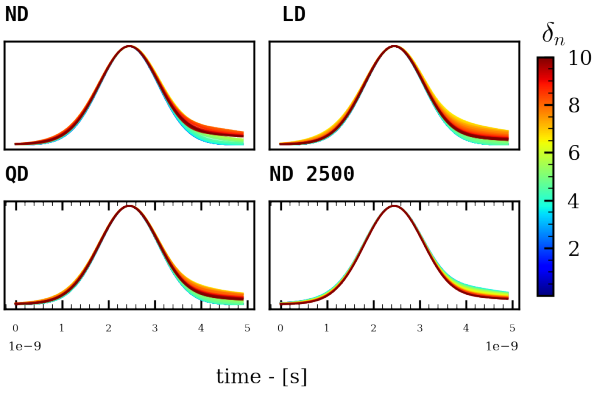

Figure 2.4: For all density profile, the pulse shape is getting broader and broader for large perturbations, and the delay is getting larger and larger. This is due to the presence of multiple scattering, and dispersive effects. This will be characterized further by the study of the mean skewness of the pulse shape.

One way to vizualize that is plotting the distribution of some parameters of the pulse shape for different perturbation amplitude. Here we choose to study the rms and the amplitude of the pulse, Indeed, it allows to the beahavior of the pulse width and height during the linear-non linear transition. This is showm in the following figure. This type of plots are called violins plot, where filled zone stands for the distribution of the random variable, calculate over every samples.

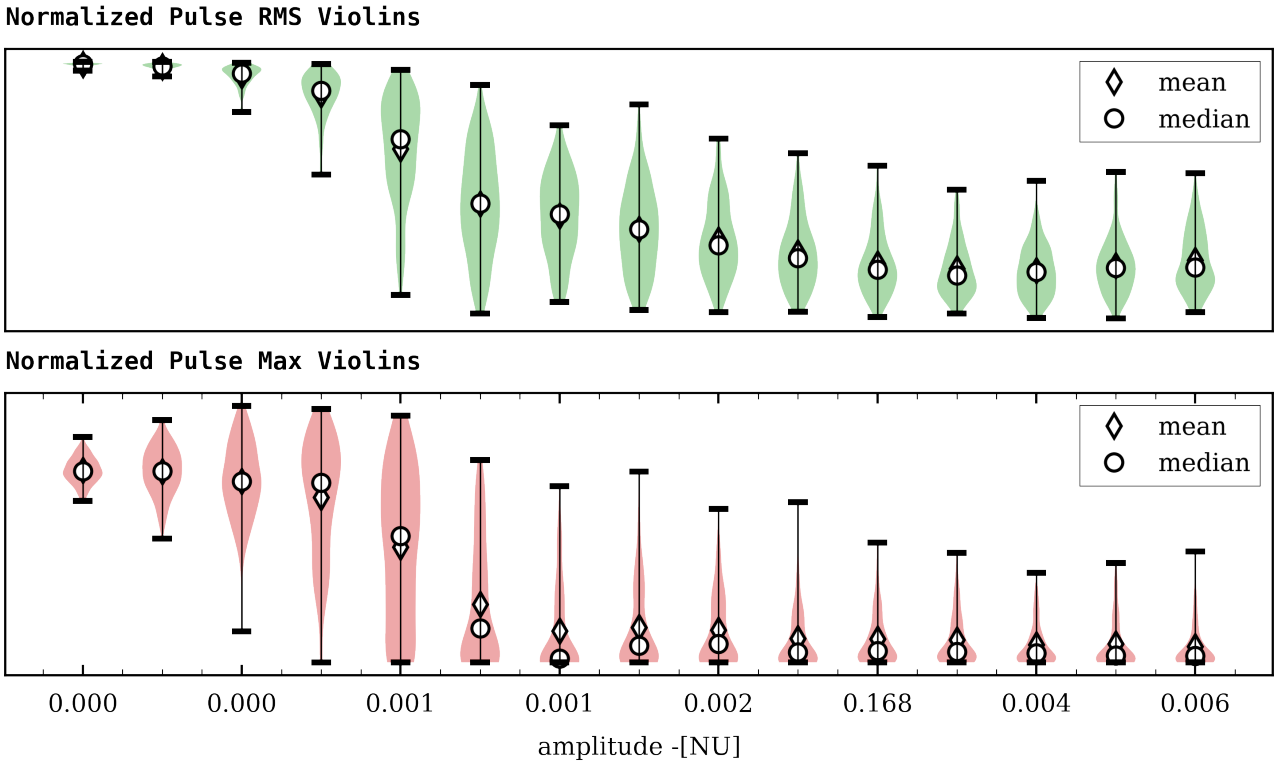

Figure 2.5: Here we plot the distribution of the pulse rms and amplitude for different perturbation amplitude, for the linear profile background profile **LD**. The distribution of the pulse rms and amplutude is getting broader and broader during the transition regime, this is due to randomness introduced by the perturbations, which seems to remains at large amplitudes, even if the distribution is getting quite constant. Lets also note that the mean of both distribution is getting smaller due to presence of multiple scattering, reaching a plateau at high turbulence ampliude.

The characteristic turbulence amplitude scale for the pulse shape transition seems to be the first critical value with $\delta n \approx 1e^{-3}$. Thanks to this study, we can unearth a way of characterizing the transition regime, using the pulse shape for multiple background profiles. For deeper insights about the pulse transition regime, we can study the skewness of the pulse shape, which should give us more information about the "broader and broader" distrubution of the pulse shape. Note that we are talking about the transition regime of the pulse shape, since the transition regime regarding the delay seems to appear at much larger amplitude at the second critical value $\delta n \approx 1e^{3}$ ax shown in Fig.2.3.

One important question we have to solve is the following, which metrics is the most relevant to characterize the transition regime. This will help us, to build a relevant datasets to tackle the non linear regime.

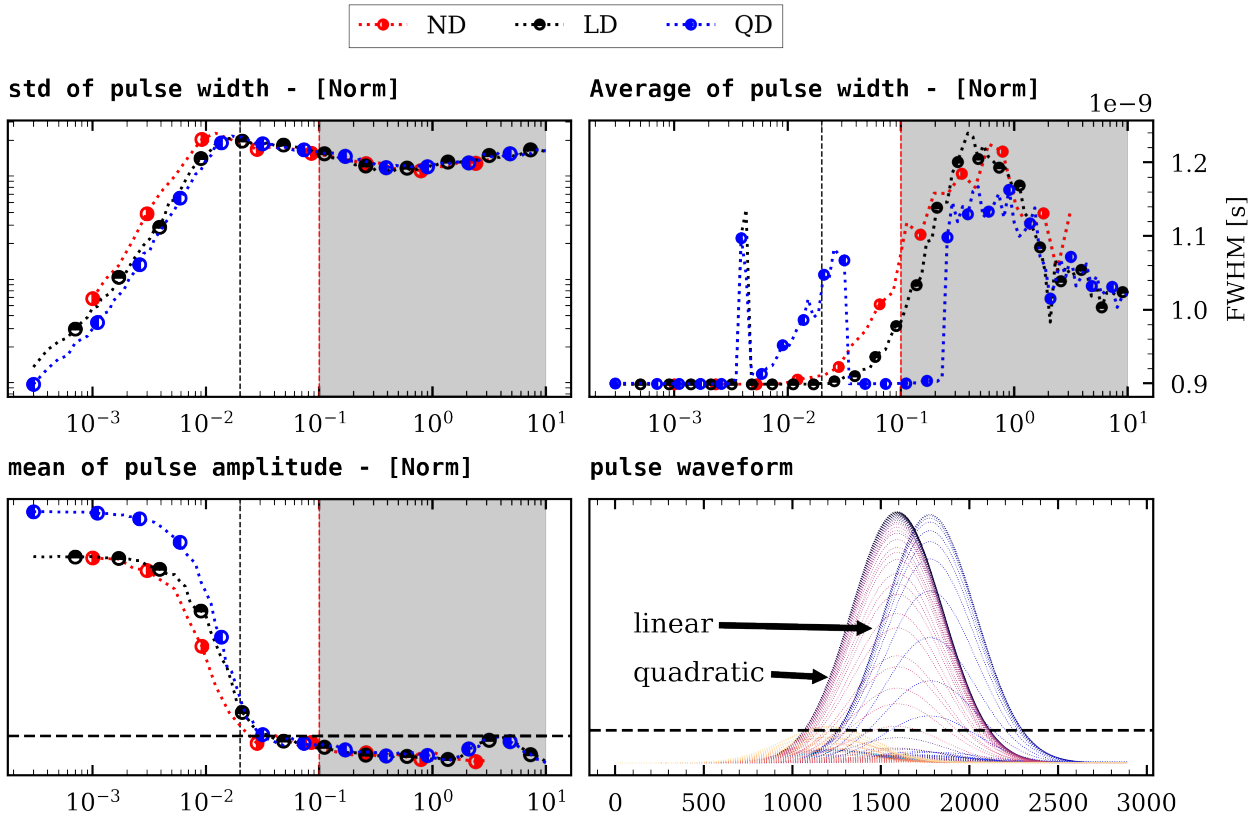

Figure 2.6: Here we plot three differents metrics to characterize the pulse shape, the std of the pulse width, which is increasing (WHY), the average pulse width is increasing as intended due to the superposition of multiple scattered pulse, for the mean pulse amplitude, it's decreasing for the same causes, however let's note that after the transition regime the mean pulse amplitude seems to increase again reaching a maximum at the amplitude value 5, the linearized turbulence turbulence density profile is also decayed from the simple linear background profile. This is easily understandable since we decrease the mean density turbulence amplitude in the plasma by linearizing the perturbation profile. One final thing to remark is the decay between the quadratic and the linear delays, indeed the quadratic profile has a little advance over the linear one. This is pssibly due to the concace shape of the background quadratic profile. Indeed, thanks to the concavity, it's much easier to turbulence to reach the cut-off layer, and to perturb it.

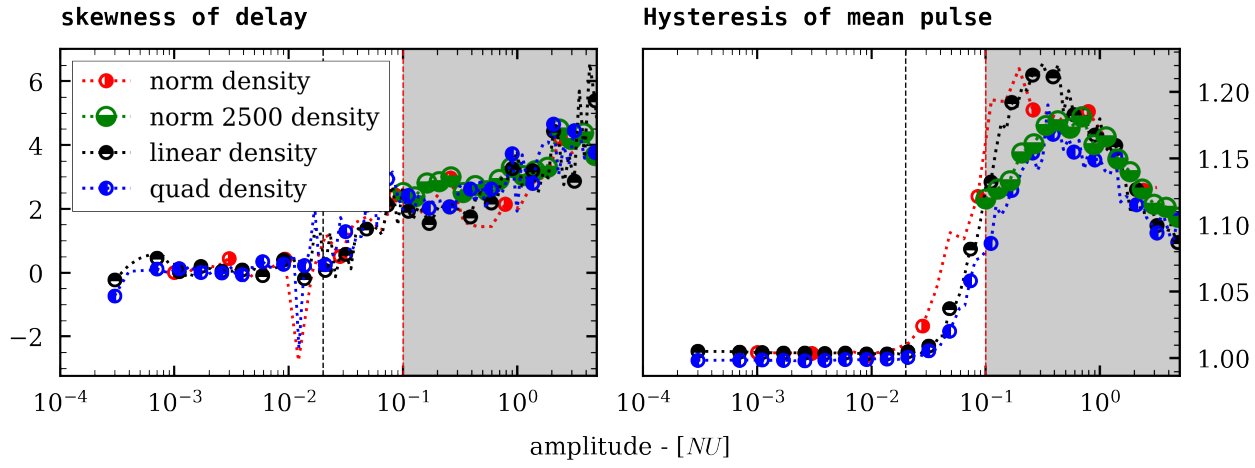

Figure 2.7: skewness of the delay shape, for different background profile, and perturbation amplitude. The skewness is getting larger and larger for large perturbations, this is due to the presence of multiple scattering, and dispersive effects. The hysteresis of the pulse is calculating using the ratio of the right area over the left area of the pulse, this allows to see the asymmetry of the pulse shape which is a measurement of the skewness of the pulse. The true Skewness of the pulse does not unearth smoothly the transition regime, this is why it is not tackled here.

3 Gaussian fitting of the pulse

On way to see the deformation of the gaussian pulse is to track the relative error of the gaussian pulse with a gaussian fit. Furthemore, it allows to study the true gaussian standard deviation, mean and amplitude. This is shown in the following figure, where we plot the relative error of the gaussian fit, and the gaussian fit

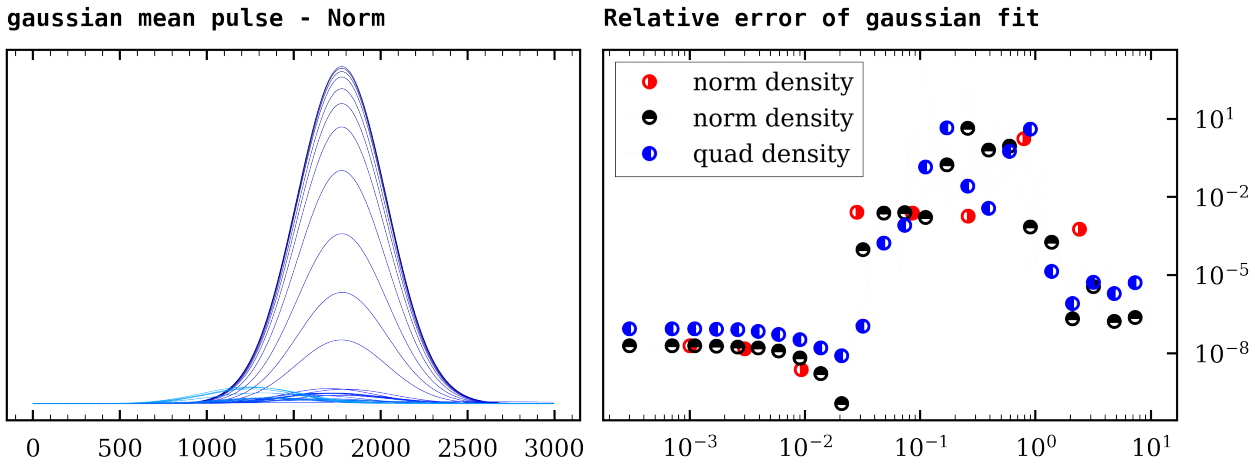

Figure 2.8: The relative error of the Gaussian fit (residuals ponderated by the size of the respective pulse amplitude) is getting large for the transition zone of the pulse shape, and seems to decline for very large turbulence. However we have to find smooth metrics to characterize the transition, and not a pseudo-random one to have better predictions in the next part. The gaussian parameters are also good quandidates and are plotted in the next figure

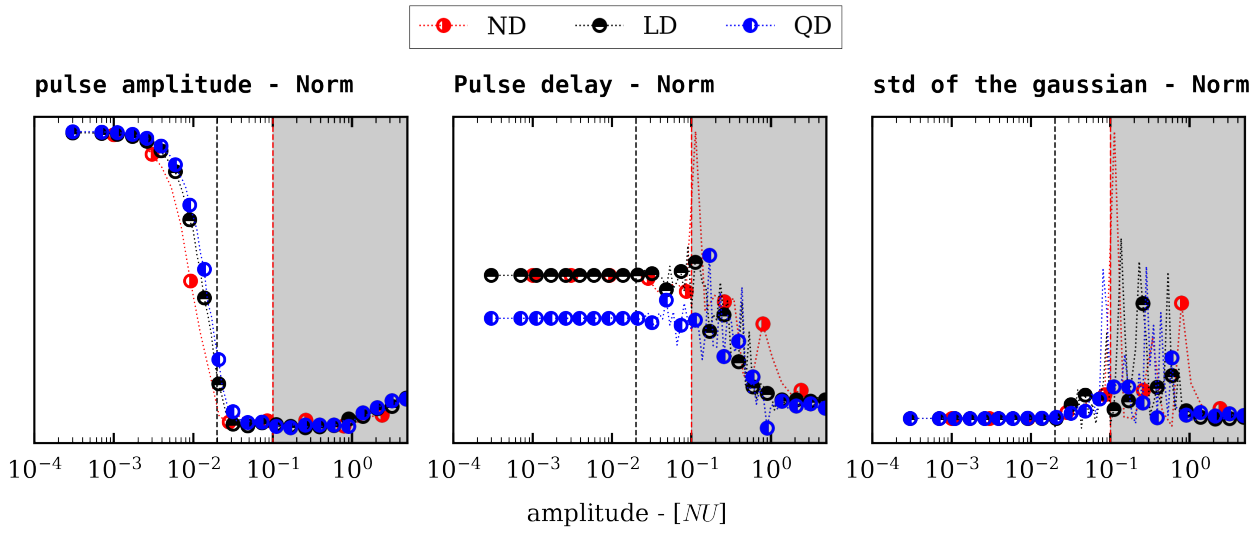

Figure 2.9: Gaussian pulse delay and standard deviation have chaotic behavior during the transition regime, this made them not relevant candidate for the next study. However lets note that the gaussian pulse ampliutde, have quite a smooth behavior, but unearth a plateau during the non linear linear transition, which might not ne a good option, even if at large amplitude we capture the same behavior as for the non gaussian amplitude. In a much cleaner way, indeed it's clearly increasing, this might be interesting to study the highly non linear regime.

IV Model collapses

As shown previously, the 1D model collapses for large perturbations. The goal of this chapter is to facilitate the deduction of the perturbations properties just from the typical study of the delayed pulse. Our goal will be to predict the perturbation amplitude, their typical correlation length and the original delay of the probing wave τ_0 without any perturbation. Using previous results, it might be quite simple to isolate the original delay and the turbulence amplitude, but the correlation length is a more difficult parameter to isolate, and seems to play a great role in the pulse properties.

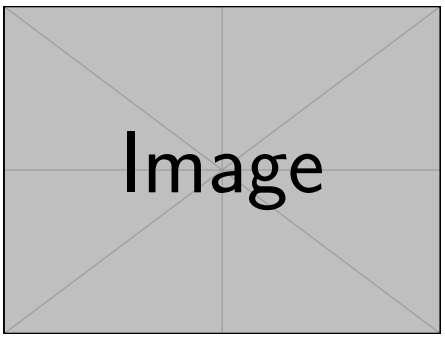

Figure 2.10: Explanation of τ_0

To deal with these multiple parameters, we will use a machine learning approach, trained on a datasets of simulated pulse shape, and delay for multiple ranges of value of δn, l_{cx}, l_{cy} and beam size ro. To build this datasets we will based our apporach on the previous results, where we extracted the best hyperparameters candidate for both computations speed and accuracy. The datasets will be built using the linear normalized perturbation profile, and a number of sample $N_s = 500$, the τ_0 will be compute for each combination of parameters, even if it should not depend on correlation lengths and ampitudes. And this for 100 samples.

V Datasets building

Parameters range			
δn	l_{cx}-[cm]	l_{cy}-[cm]	ro-[cm]
$[1e^{-3}, 1]$	$\{1, 0.5\}$	$\{0.5, 2, 30\}$	$\{1, 4, 10\}$

This makes a combination of 216 points in a 4D space, which is a reasonable number of points to train a machine learning model. However lets note that this multidimensional output space, brings some subtitlities to the problem. First what's the best pulse metrics to use for the training as input data.

3

Mathematical appendix

1. Gaussian perturbation integral

$$\tau_d = \frac{2}{c}\int_0^L \frac{dx}{\sqrt{1-\frac{x}{L}-\frac{\delta n \exp\left(-\frac{(x-L)^2}{8l_{cx}^2}\right)}{n_c}}}$$

The first assumption that we can made is that away from $L-l_{cx}$ the perturbation is negligible, thanks to that we can expand the integral to the following :

$$\tau_d = \frac{2}{c}\int_{L-l_{cx}}^L \frac{dx}{\sqrt{1-\frac{x}{L}-\frac{\delta n \exp\left(-\frac{(x-L)^2}{8l_{cx}^2}\right)}{n_c}}} + \frac{2}{c}\int_0^{L-l_{cx}} \frac{dx}{\sqrt{1-\frac{x}{L}}}$$

Let's focus on the first integral, we can expand the exponential to the first order, and we obtain the following :

$$\begin{aligned}
&\frac{2}{c}\int_{L-l_{cx}}^L \frac{dx}{\sqrt{1-\frac{x}{L}-\frac{\delta n \exp\left(-\frac{(x-L)^2}{8l_{cx}^2}\right)}{n_c}}} \\
&\approx \frac{2}{c}\int_{L-l_{cx}}^L \frac{dx}{\sqrt{1-\frac{x}{L}-\frac{\delta n}{n_c}(1-\frac{(x-L)^2}{8l_{cx}^2})}} \\
&\approx \frac{2}{c}\int_0^{l_{cx}} \frac{dx}{\sqrt{\frac{x}{L}-\frac{\delta n}{n_c}(1-\frac{x^2}{8l_{cx}^2})}}
\end{aligned}$$

Now we can introduce the x_0 and K_1 constants defined by :

$$x_0 = \sqrt{8\frac{n_c}{\delta n}l_{cx}^2} \text{ and } K_1 = \sqrt{\left(\frac{x_0}{2L}\right)^2 - 8\left(\frac{l_{cx}}{x_0}\right)^2}$$

which leads to the following canonical form of the integral :

$$\begin{aligned}
&\frac{2}{c}\int_0^{l_{cx}} \frac{dx}{\sqrt{(\frac{x}{x_0}-\frac{x_0}{2L})^2 - K_1^2}} \\
&= \frac{2}{c}x_0 \int_{-\frac{x_0}{2LK_1}}^{(\frac{l_{cx}}{x_0}-\frac{x_0}{2L})/K_1} \frac{dx}{\sqrt{x^2-K_1^2}} \\
&= \frac{2}{c}x_0 \int_{-\frac{x_0}{2LK_1}}^{(\frac{l_{cx}}{x_0}-\frac{x_0}{2L})/K_1} \frac{dx}{\sqrt{x^2-1}} \\
&= \frac{2}{c}x_0 \left[\log\left(\sqrt{x^2-1}+x\right)\right]_{-\frac{x_0}{2LK_1}}^{(\frac{l_{cx}}{x_0}-\frac{x_0}{2L})/K_1} \\
&= \frac{2}{c}x_0 (\log\left(\sqrt{(\frac{K_2}{K_1})^2-1}+\frac{K_2}{K_1}\right) \\
&- \log\left(\sqrt{(\frac{K_2^*}{K_1})^2-1}+\frac{K_2^*}{K_1}\right))
\end{aligned}$$

With $K_2 = \left(\frac{l_{cx}}{x_0}-\frac{x_0}{2L}\right)$ and $K_2^* = -\frac{x_0}{2L}$.